TESTING AND ANALYSIS TO DETERMINE THE SHELL THICKNESS REQUIRED TO PREVENT PUNCTURE

D. J. Ammerman, H. D. Radloff, and E. J. Eifert

Sandia National Laboratories, Albuquerque, New Mexico, United States of America*

INTRODUCTION

Type B radioactive material packages are required to withstand a hypothetical puncture accident of a free fall from a height of one meter onto a 15 cm diameter mild steel puncture probe. For many packages it is desirable to have this accident event not result in puncture or tearing of the outer shell of the package. The wall thickness necessary to prevent this has historically been determined by test or the use of empirical relations. This technique generally results in overly conservative designs, but the degree of conservatism is uncertain. The use of modern finite element codes to determine package response to puncture accidents can result in designs that are both safe and economical. The work reported in this paper is aimed at developing a method to analytically determine the wall thickness required to prevent puncture. For designers and regulators to have confidence in this analytical method, however, it must be benchmarked against test results. A series of tests has been conducted with differing shell thicknesses, shell materials of mild steel and stainless steel, and shell backing materials of lead, foam, and air. The results of these tests have been compared with pre-test analytical predictions of the response obtained from the non-linear transient dynamic finite element program PRONTO-2D. From this comparison it can be seen that the finite element method can accurately predict the response of packages to puncture accidents. This implies that an analytical technique based on the finite element method can be used to design packages having known response and margin of safety against tearing of the outer shell. In addition, the analytical technique can accurately predict the deformed shape of the package following the test. This may be important for subsequent calculations, such as external dose and heat input during a thermal event.

TESTS PERFORMED

An experimental test series using 1/3 scale models was conducted to investigate two shell materials and three backing materials. These test units were approximately 44 cm in diameter. Figure 1 is a schematic of the test fixture which allowed the impact plates and the backing materials to be reconfigured for each test. The schematic on the left corresponds to configurations with backing materials, while the schematic on the right represents cases with no backing material (air backed). For the tests involving backing material, the backing material, a stiff backing plate and a spacer ring were sandwiched between the test plate and the transition piece. For the test configurations without any backing material, the test ring and plate were bolted directly to the transition piece. The transition piece / test ring assembly was bolted to a large steel weight. The mass of each test unit assembly was approximately 1000 kg.

* Sandia is a multiprogram laboratory operated by Sandia Corporation, a Lockheed Martin Company, for the United States Department of Energy under Contract DE-AC04-94AL85000.

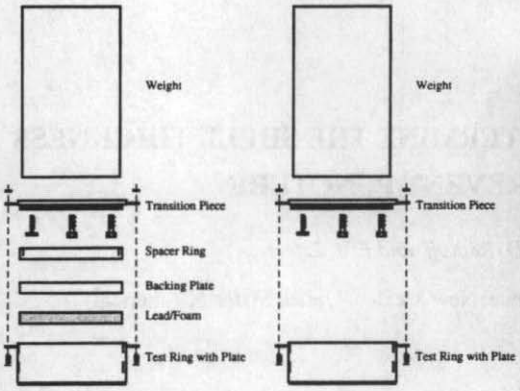

Figure 1: Schematic of test fixture configurations.

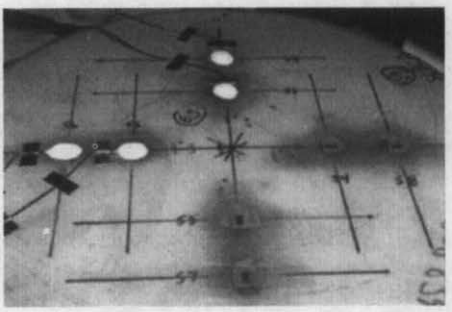

Figure 2: Strain gage placement on test units.

Four test specimens were prepared for each of the six possible combinations of plate and backing material. Two specimens had the predicted critical plate thickness, a third specimen was one standard gauge thickness thinner, and a fourth specimen was one standard gauge thicker. Table 1 presents the plate material, backing material, and plate thickness represented in the test series. Each test unit was instrumented with eight uniaxial strain gages mounted as shown in Figure 2. Four strain gages were equally spaced around the intended impact point at a radius of 7.6 cm. The remaining four were mounted at a radius of 12.7 cm. In order to measure strains due to plate bending, all of the strain gages were oriented with the active direction of the grid aligned radially toward the impact point.

Table 1: Test Matrix of Plate Thicknesses in Inches (cm)

Plate material	Backing material	1 Specimen	2 Specimens	1 Specimen
304-SS	Lead	5/16 (0.794)	1/4 (0.635)	3/16 (0.476)
1040-CS	Lead	3/8 (0.953)	5/16 (0.794)	1/4 (0.635)
304-SS	Foam	1/4 (0.635)	3/16 (0.476)	1/8 (0.318
1040-CS	Foam	5/16 (0.794)	1/4 (0.635)	3/16 (0.476)
304-SS	Air	3/16 (0.476)	1/8 (0.318)	.105 (0.267)
1040-CS	Air	1/4 (0.635)	3/16 (0.476)	1/8 (0.318)

Figure 3 shows a partially assembled test unit with the test ring and foam backing material visible in the left side of the figure and with the backing plate and spacer ring installed in the right side of the figure. This assembly would then be bolted to the large weight that simulates the remainder of the package via the four dog-ears shown in the figure.

For each plate / backing material combination considered, the test unit with the calculated critical plate thickness was tested and the plate examined for puncture. If the plate did not puncture, the drop height was increased slightly and the second unit having the same plate

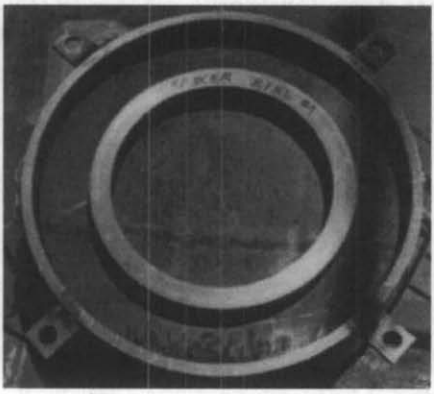

Figure 3: Test unit assembly showing the test ring, backing material, backing plate, and spacer ring.

thickness tested. If the plate did puncture, the drop height was decreased slightly and the second unit tested. If the plate with the critical thickness punctured, there was no need to test the thinner plate. Similarly, if the plate with the critical thickness did not puncture, there was no need to test the thicker plate.

Figures 4 and 5 show post-test views from the inside and outside, respectively, of the 1/4 inch (0.635 cm) 304-SS plate backed with lead dropped from a height of one meter. Plastic flow and incipient plate puncture are clearly visible. This is the thickness at which the finite element model predicted that strains in the steel shell would reach the point where tearing is likely to occur.

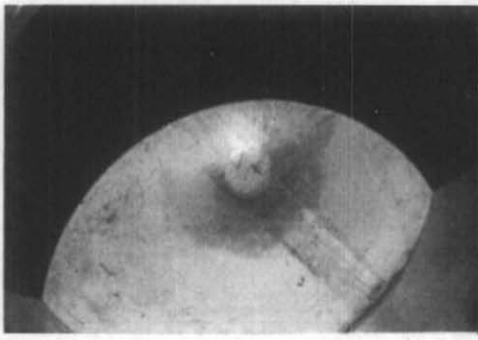

Figure 4: View from inside the test unit.

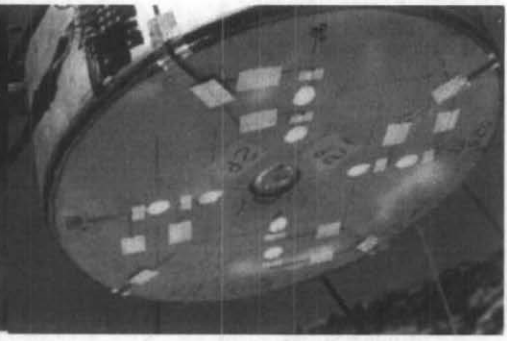

Figure 5: View from outside the test unit.

FINITE ELEMENT ANALYSES

A series of finite element analyses was performed to calculate the plate thicknesses required to induce tearing. The analyses were performed using the explicitly integrated finite element code PRONTO-2D (Taylor and Flanagan 1987). Axisymmetric models were developed to include very accurate depictions of the plate, backing material, and loading apparatus in order to match

the experimental configuration as closely as possible. Figure 6 presents model geometry showing the punch, plate, backing material, stiffening plate, standoff region, ring, transition plate, and steel mass.

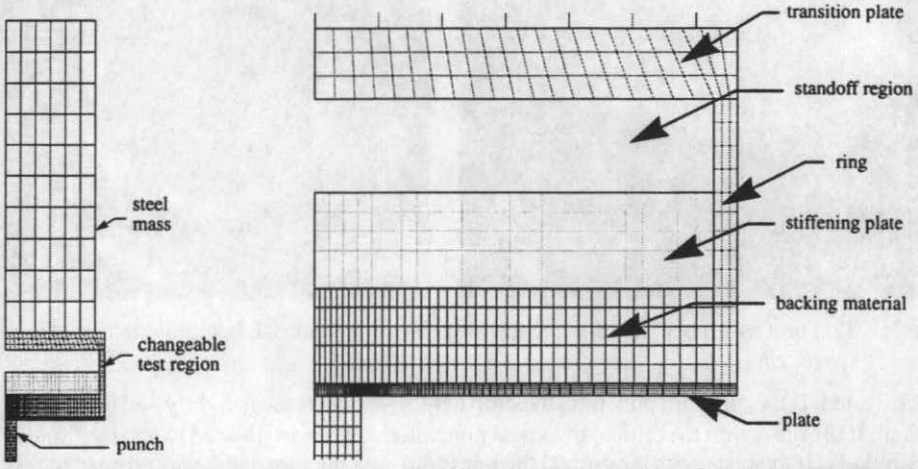

Figure 6: Axisymmetric finite element model geometry. On the left is the complete model, on the right is an enlargement of the changeable test region.

An isotropic elastic/plastic power-law hardening model (Stone et al. 1990) was used to represent the lead, plate materials, and ring. The transition plate, stiffening plate, steel mass, and punch were modeled using an elastic model. The foam was modeled using the new foam model in PRONTO-2D. Table 2 summarizes all of the required properties associated with each material.

Table 2: Material properties used in analysis

Property	304-SS	1040-CS	Lead	Foam
Density (g/cm^3)	7.9	7.9	11.4	1.6
Young's Modulus (MPa)	193	200	13.8	0.3
Poissons Ratio	0.27	0.30	0.27	0.30
Yield Stress (KPa)	138	358	5.5	3450 (A)
Ultimate Stress (KPa)	483	483	-	1380 (B)
Hardening Constant (KPa)	1329	1193	5.5	6895 (POLY)
Hardening Exponent	0.74819	0.54	0.5	0.1 (P_0)
Luder's Strain	-	-	0.3	0.8 (ϕ)
Assumed Failure Strain (not part of model)	0.8	0.5	-	-

In the analysis, the bottom of the punch was fixed and the remainder of the model was given an initial velocity toward the punch. The initial impact velocity was 4.46 m/sec which corresponds to a one-meter drop. The plate impacted the punch at time=0 and the impact event was assumed to be completed when the total kinetic energy of the system reached a minimum value. If the maximum equivalent plastic strain in the plate material exceed the assumed strain at failure from Table 2, it was assumed the plate would tear in a test. No effort was made to model the tearing or post-tearing behavior of the specimen.

Figure 7 shows the equivalent plastic strains of the impact plate in a local area near the punch for the cases of 304-SS plate material with lead and foam backing material. These figures reveal a very similar plate response, although the critical plate thicknesses shown are different. The maximum equivalent strain is located at the bottom of the plate at a radius slightly larger than the punch. Each plate also shows a sharp bend directly at the edge of the punch with a very smooth transition to a flat undeformed shape approximately halfway between the punch and plate edge.

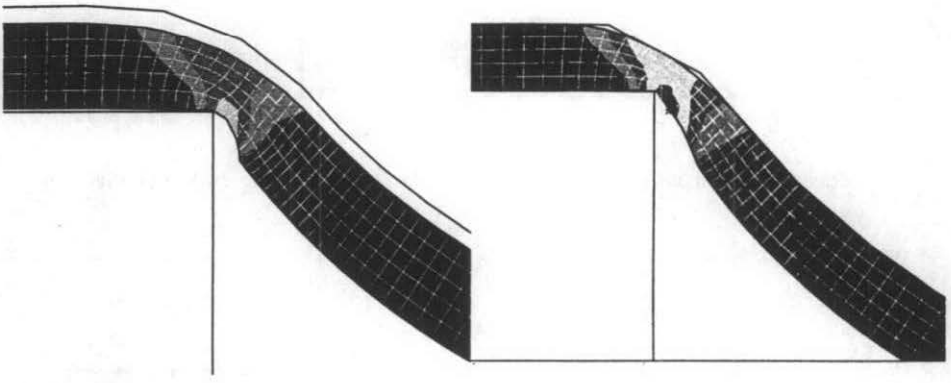

Figure 7: Strains in 304-SS plate with lead backing and with foam backing.

COMPARISON OF RESULTS

From the preceding sections it can be seen that the qualitative results from the tests and the finite element analyses are similar. In this section, these results will be compared quantitatively. Figure 8 shows comparisons of deflected shapes for three of the tests with 304-SS plate: one with no backing, one with foam backing, and one with lead backing. The measured data include deflections along two orthogonal diameters. The data in the two directions and for both sides of each direction are not identical due to slight off-center locations of the impact point. The cases shown are for the thicknesses where the finite element model strains were at the point of failure. In the tests, the plate with air backing was punctured and the other two were not. Comparing the test and analysis results, it can be seen that in the case with no backing the finite element results predict greater deformation than observed in the test. This is because the tearing of the test specimen prevented additional global deformation, while tearing was not included in the finite element model. For the other two backing materials, the measured and calculated deflections agree very closely. In the case with foam backing the calculated deformations away from the punch are slightly less than those measured, indicating a slight overprediction of the stiffness of the foam.

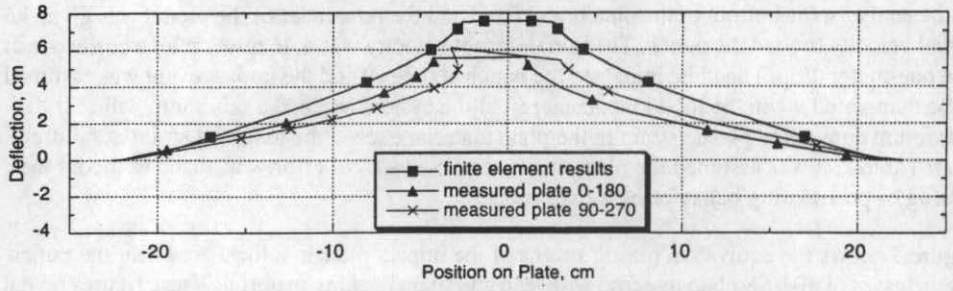

Results for the case with no backing and 1/8 inch (0.32 cm) thick plate

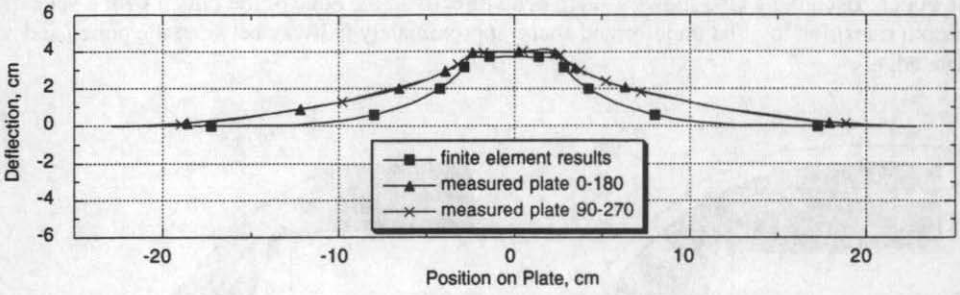

Results for the case with foam backing and 3/16 inch (0.48 cm) thick plate

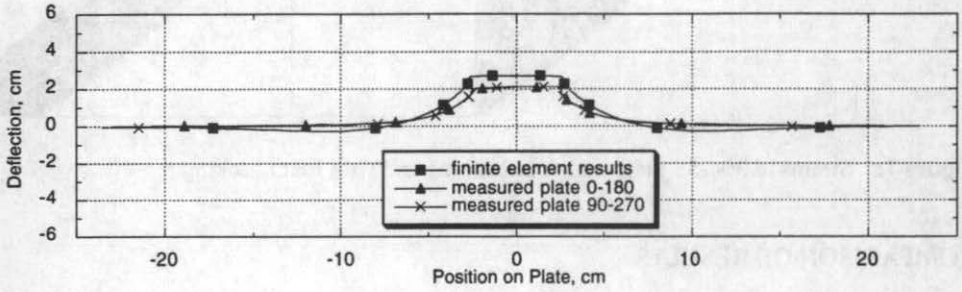

Results for the case with lead backing and 1/4 inch (0.64 cm) thick plate

Figure 8: Comparison of measured and calculated deformed shapes for 304-SS plates with various backing materials.

The results from Figure 8 indicate the finite element method was able to predict the final deformations in the plates that did not experience puncture. Comparison of the time history for the strain gages and predicted strains demonstrate whether the finite element method was also able to predict the rate of the deformations. Figure 9 shows a comparison between the finite element calculated strains and the strain gage results for the case with 5/16 inch (0.79 cm) thick 1040-CS plate with foam backing material. The scatter in the strain gage data is due to the slight off-center location of the impact point. For both gage alignments the finite element calculated strains are slightly higher than the measured strains during the early portions of the impact. The

peak calculated strain occurs at about 10.5 ms into the impact, while the peak measured strain does not occur until about 16 ms into the impact. This response is another indication that the stiffness of the foam in the finite element model is slightly high.

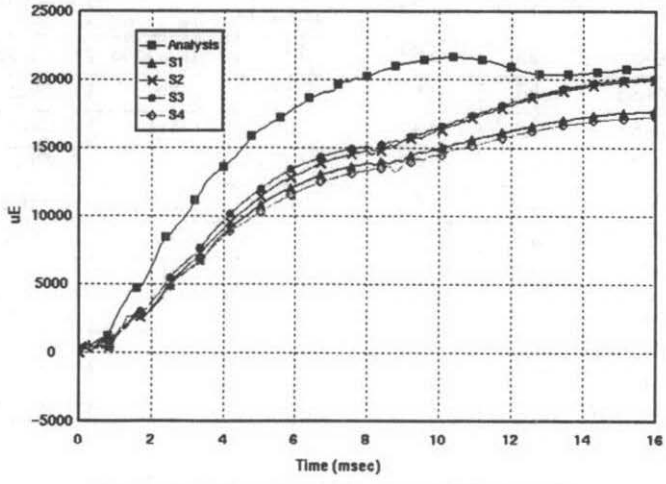

Strains at 7.6 cm from the center of the punch.

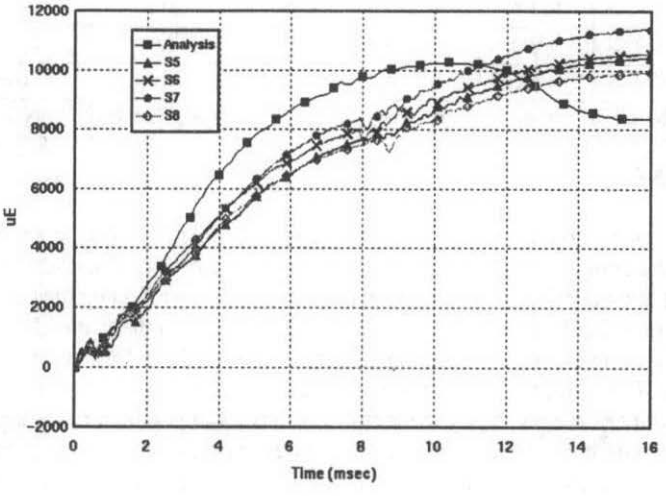

Strains at 12.7 cm from the center of the punch.

Figure 9: Comparison of finite element and measured strain histories for the case with 5/16 inch (0.79 cm) thick 1040-CS plate with foam backing material.

The ability of the finite element method to predict the thickness of plate required to prevent puncture can be seen from the summary results in Table 2. This table shows the drop height and puncture results for each test, along with the finite element prediction for the results. As can be seen, the finite element predicted the results of almost all of the tests correctly, with only the case with 1040-CS and no backing having a large deviation.

Table 3: Summary of Results

Plate Material	Backing Material	Thickness (cm)	Drop Height (meters)	Puncture?	FEM prediction
304-SS	lead	0.635	1.0	No, Close	Close
304-SS	lead	0.635	1.14	Yes	Yes
304-SS	lead	0.476	1.0	Yes	Yes
304-SS	foam	0.476	1.0	No	Close
304-SS	foam	0.476	1.22	No	Yes
304-SS	foam	0.318	1.0	Yes	Yes
304-SS	none	0.476	1.0	No	No
304-SS	none	0.318	1.0	Yes	Close
1040-CS	lead	0.953	1.0	No	No
1040-CS	lead	0.794	1.0	No, Close	Close
1040-CS	lead	0.794	1.04	Yes	Yes
1040-CS	lead	0.635	1.0	Yes	Yes
1040-CS	foam	0.794	1.0	No	No
1040-CS	foam	0.635	1.0	Yes	Close
1040-CS	foam	0.635	0.89	Yes	No
1040-CS	none	0.635	1.0	Yes	No
1040-CS	none	0.476	1.0	Yes	Close
1040-CS	none	0.476	0.48	Yes, Barely	No

CONCLUSIONS

The finite element method can be used to obtain a good prediction of the plate thickness required to prevent punch through. As can be seen from the results of the testing program, the ductility of the plate material and the material backing it have an effect on the thickness required to prevent puncture. Both of these effects are accounted for with the finite element method. Additionally, the finite element method can be used to predict the deformations observed during puncture events. This information is important to assess the effect of the puncture test on the shielding capability of the package. The factor of safety against puncture for a given package can be determined with the finite element method by either running analyses with progressively higher puncture energies (initial drop height) until failure is observed, or by comparing the maximum strain in the plate material to its failure strain.

REFERENCES

Taylor, L. M. and Flanagan, D. P., "PRONTO 2D: A Two-Dimensional Solid Dynamics Program", SAND86-0594, Sandia National Laboratories, Albuquerque, NM, USA (March 1987).

Stone, C. M., Wellman, G. W., and Krieg, R. D., "A Vectorized Elastic-Plastic Power Law Hardening Material Model Including Luders Strain", SAND90-0153, Sandia National Laboratories, Albuquerque, NM, USA (1990).